

Full length article

Application of Dempster-Shafer theory of evidence model to geoelectric and hydraulic parameters for groundwater potential zonation

Kehinde Anthony Mogaji^{a,b,*}, Hwee San Lim^b^a Department of Applied Geophysics, Federal University of Technology, P.M.B. 704, Akure, Nigeria^b School of Physics, Universiti Sains Malaysia, 11800 Penang, Malaysia

ARTICLE INFO

Article history:

Received 10 October 2017

Revised 6 December 2017

Accepted 31 December 2017

Available online 8 January 2018

Keywords:

ROC

DS-EBF

Resistivity imaging

Groundwater - potential

Uncertainty

Dar – Zarrowk Parameter

Geoelectric

Hydraulic

ABSTRACT

The application of a GIS – based Dempster – Shafer data driven model named as evidential belief function EBF- methodology to groundwater potential conditioning factors (GPCFs) derived from geophysical and hydrogeological data sets for assessing groundwater potentiality was presented in this study. The proposed method's efficacy in managing degree of uncertainty in spatial predictive models motivated this research. The method procedural approaches entail firstly, the database containing groundwater data records (bore wells location inventory, hydrogeological data record, etc.) and geophysical measurement data construction. From the database, different influencing groundwater occurrence factors, namely aquifer layer thickness, aquifer layer resistivity, overburden material resistivity, overburden material thickness, aquifer hydraulic conductivity and aquifer transmissivity were extracted and prepared. Further, the bore well location inventories were partitioned randomly into a ratio of 70% (19 wells) for model training and 30% (9 wells) for model testing. The synthesized of the GPCFs via applying the DS – EBF model algorithms produced the groundwater productivity potential index (GPPI) map which demarcated the area into low – medium, medium – high and high potential zones. The analyzed percentage degree of uncertainty for the predicted lows potential zones classes and mediums/highs potential zones classes are >10% and <10%, respectively. The DS theory model-based GPPI map's validation through ROC approach established prediction rate accuracy of 88.8%. Successively, the determined transverse resistance (TR) values in the range of 1280 and 30,000 $\Omega \text{ m}^y$ for the area geoelectrically delineated aquifer units of the predicted potential zones through Dar – Zarrowk Parameter analysis quantitatively confirm the DS theory modeling prediction results. This research results have expand the capability of DS – EBF model in predictive modeling by effective uncertainty management. Thus, the produced map could form part of decision support system reliable to be used by local authorities for groundwater exploitation and management in the area.

© 2018 Production and hosting by Elsevier B.V. on behalf of National Research Institute of Astronomy and Geophysics. This is an open access article under the CC BY-NC-ND license (<http://creativecommons.org/licenses/by-nc-nd/4.0/>).

1. Introduction

The spatial prediction of groundwater potential using the standard method is important for groundwater resources management (Rahmati et al., 2016; Mogaji and Omobude, 2017). Groundwater

* Corresponding author at: Department of Applied Geophysics, Federal University of Technology, P.M.B. 704, Akure, Nigeria.

E-mail addresses: kamoaji@futa.edu.ng (K.A. Mogaji), hslim@usm.my (H.S. Lim).
Peer review under responsibility of National Research Institute of Astronomy and Geophysics.



being a hidden subsurface treasures resource not easily seen with the naked eyes is very difficult to quantify potentially. Subsequently, planners and hydrological engineers have resolved to engage the efficacy of the predictive standard methods in groundwater potentiality mapping. Indeed, this has contributed immensely to managing groundwater resource sustainably (Pourghasemi and Beheshtirad, 2015). This precious natural resource often served as a driven resource in all works of life such as industrial and agricultural purposes (Pradhan, 2009; Ayazi et al., 2010; Manap et al., 2013; Neshat et al., 2014; Nampak et al., 2014). Consequently, the increasing demand for such natural resource in all climatic regions in the world by the way of rapid population growth, urbanization, drought among others, cannot be over emphasized (Magesh et al., 2012; Todd and Mays, 2005; Oikonomidis et al., 2015). Therefore, the optimal maximization of

this vital natural resources i.e. potentiality evaluation requires efficient management (Oikonomidis et al., 2015).

Recently, the usage of the multi-criteria predictive standard methods has been reportedly a good alternative in environmental decision making venture (Akinlalu et al., 2017; Oni et al., 2017; Mogaji and Lim, 2017). Thus some renowned GIS – based spatial integration models such as weights-of-evidence, probabilistic frequency ratio, Shannon's entropy, logistic regression, artificial neural network, analytical hierarchy process and evidential belief function have been fully engaged in groundwater potential mapping (Al-Abadi, 2015a, Corsini et al., 2009; Lee et al., 2012a,b,c; Pourtaghi and Pourghasemi, 2014; Naghibi et al., 2014; Davoodi

Moghaddam et al., 2013; Oh et al., 2011; Ozdemir, 2011a, 2011b; Naghibi et al., 2014; Corsini et al., 2009; Lee et al., 2012b; Kaliraj et al., 2014; Mogaji, 2016; Nampak et al., 2014; Mogaji et al., 2015a). However, it is important to note that the commonest groundwater potential conditioning factors (GPCFs) often used in these priors studies include lineament density, lineament intersection density, drainage density, slope, lithology and rainfall, etc. However, the studies on the use of the geophysical and hydrogeological inclined GPCFs such as (aquifer resistivity, aquifer thickness) and (transmissivity and storativity), respectively in spatial predictive mapping of groundwater potentiality are few. According to Sener et al. (2005) and Madan et al. (2010), these latter GPCFs

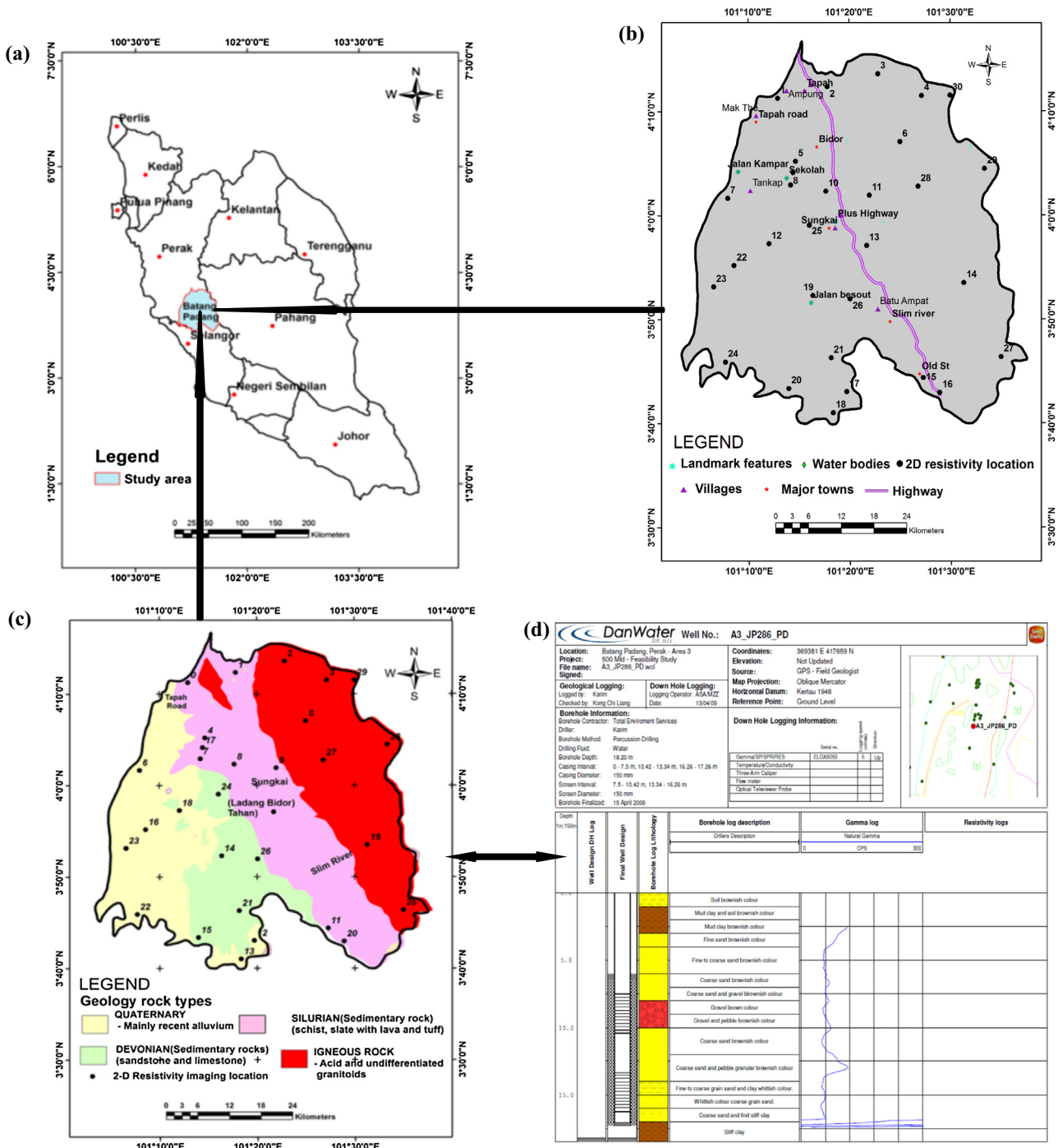


Fig. 1. The study area description materials showing a: map of Peninsular Malaysia; b: site location map depicting the 2D Resistivity imaging location point; c: the area geologic rock types map and d: typical borehole litho – log of the area.

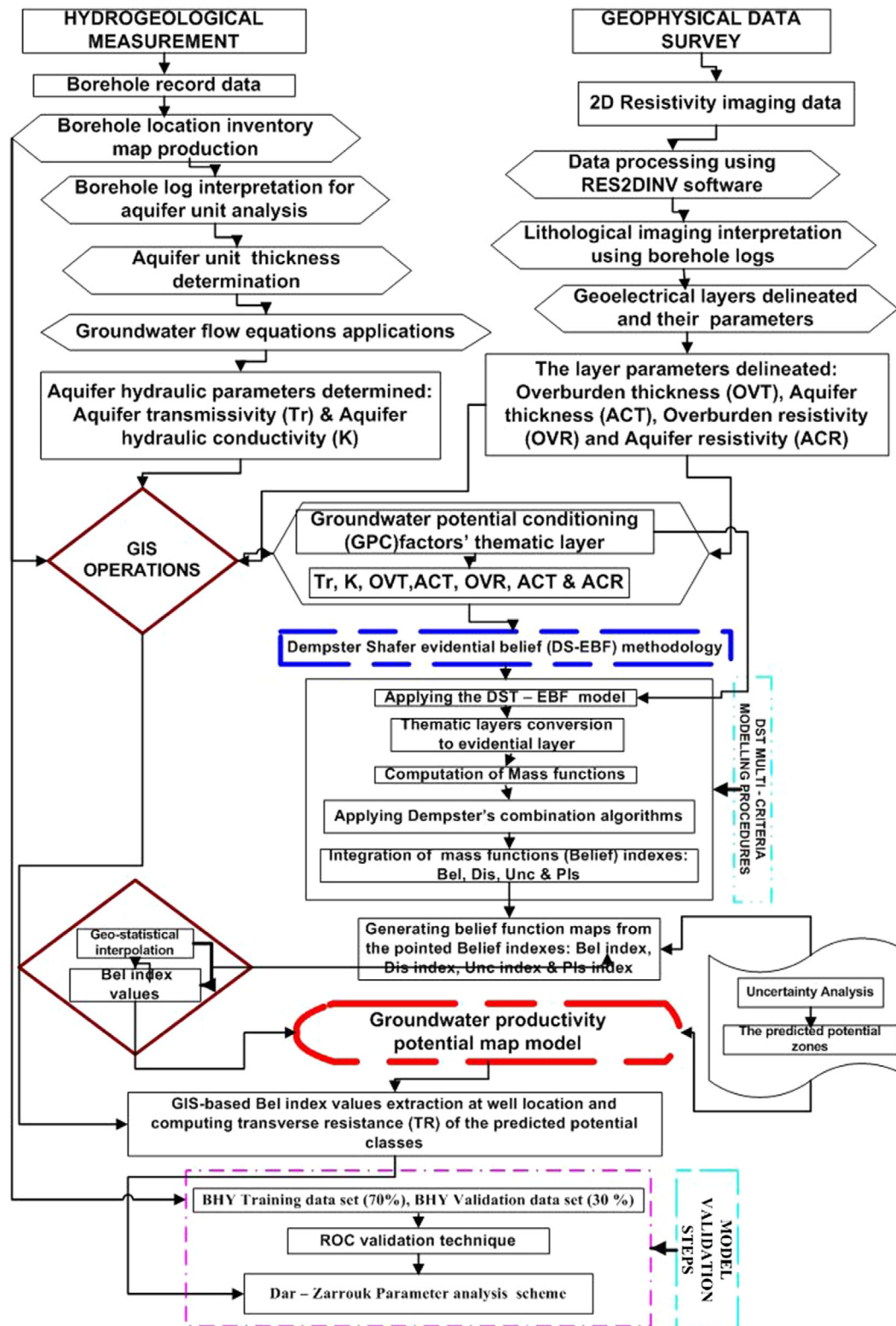


Fig. 2. The methodological flowchart adopted for the study.

have direct bearing and an in situ contact with the subsurface fluid flow mechanism. Moreover, among the often used multi-criteria index predictive model, few studies have applied the data-driven evidential belief functions methodology.

This current research introduce the EBF model in mapping the groundwater potentiality leads at a given study area in Perak province, Malaysia. The conceptual novel of this study deals with the

construction of groundwater productivity potential index (GPPI) map via synthesizing the goelectrical and hydrogeologic data sets driven factors including overburden resistivity (OVR), overburden thickness (OVT), aquifer resistivity (ACR), aquifer thickness (ACT), hydraulic conductivity (K), aquifer transmissivity (Tr) using the proposed model algorithms. Through utilizing this model in-built degree of uncertainty relationship functionality, estimate of the

degree of uncertainty characteristics of the predicted potential zones which according to Feizizadeh et al. (2014) can provide the possibilities of measuring the level of confidence in decision making was analyzed over the promising potential zones identified in the investigated area. Further, the efficiency of the model was evaluated using the result of the reacting operating characteristics (ROC) technique and the analyzed result of the Dar – Zarrouk Parameters (DZP) determined for the area underlain aquifer formation materials. The application of Dempster – Shafer data driven evidential belief function (DS – EBF) in groundwater potentiality mapping using the subsurface derived groundwater potential conditioning geoelectric and hydraulic parameters provides originality to this study.

2. The study area description

The study area is situated in the southern region of Perak and shares boundaries with Selangor in Peninsular Malaysia. The area is bounded by longitudes 101°0'E–101°40'E and latitudes 3°37'N–4°18'N (Fig. 1). The detail of the area geography, hydrology, hydrogeology and geology (Fig. 1c) have been discussed and documented in Mogaji et al. (2015a). Literatures have generally reported that the study area is characterized to be underlain with varying aquifer types such as confined aquifer and unconfined aquifer (Mogaji et al., 2015b). The delineation and mapping of these groundwater reservoir (aquifer) conditions as well their potential productivity requires standard methods to regionally manage them for optimal groundwater resource maximization.

3. Materials and methodology

The used data in this study encompasses, the obtained borehole pumping test (BPT) measurements data (Hydrogeological measurement) and the field acquired geophysical data. Fig. 2, presents an overview of the applied DS – EBF methodology for the regional assessment of the groundwater productivity potential mapping in the study area. The approach were implemented at seven different phases: The hydrogeological measurement was staged at phase (1) where borehole pumping test (BPT) survey analysis for the purpose of groundwater wells location inventory mapping, the bore well yield record analysis, the bore litho – log interpretation (Fig. 1d) and the determination of K and Tr parameters for each occupied borehole well in the area. Phase (2) involved the regional field geophysical prospecting investigation where 2D resistivity imaging geophysical data acquisition, processing and interpretations were carried out and determination of Dar – Zarrouk Parameter (DZP) from the interpreted geoelectrical parameters (layer thickness (h) and layer resistivity (ρ)) at each occupied (Figs. 1b and 2). The application of GIS tool constituted the Phase (3), at this phase, production of thematic maps of GPCFs parameters such OVT, OVR, ACT, ACR, Tr and K were processed and also the overlay and spatial analysis between the produced GPPI map and the determined transverse resistance (TR) values were evaluated. The DS – EBF methodology details constituted Phase (4) where the EBF model theory applicability in groundwater potentiality mapping was explored. The 5th phase deals with the production of groundwater productivity potential index map for the area. The quantification of degree of uncertainty over the predicted potential zones make up Phase (6). The validation of the model results for its efficiency analysis has the 7th Phase. The details of these aforementioned phases are highlighted below.

3.1. The hydrogeology measurement phase

At this phase, the available BPT data record and borehole litho – log were analyzed. With the BPT survey, the inventory map of the

well location was prepared for the regional analysis of the area hydrogeological condition. The adopted pumping test principle in the BPT technique involved the use of Cooper and Jacob's straight-line methods for analyzing the pumping test results of the measured drawdown reading with respect to time in each drilled boreholes occupied as detailed in the study of Anomohanran (2015). Each of the drawdown readings were analyzed at each tested wells after a specific time intervals of pumping. Employing, the linear regression technique, the variables of the drawdowns on an arithmetic axis versus time on a logarithmic axis were plotted to determine the aquifer hydraulic properties such as yield rate and Tr parameters. According to Table 1, the bore wells groundwater productivity values (i.e. yield rate) in the range of 0.39–43.73 m³/h were analyzed for data driven application of the DS – EBF modeling via randomly partitioning into 70% (19 groundwater wells) as training data set while the remaining 30% (9 groundwater wells) are for the model validation. Afterward, the available borehole litho – log (Fig. 1d) were interpreted to determine the aquifer unit thickness (h). With the application of the groundwater flow equation as used in Pradhan et al. (2013), the aquifer hydraulic parameter (K) was determined. The determined values for each of the Tr and K parameters at each located borehole were processed in GIS environment to produced their thematic maps.

3.2. Field geophysical prospecting investigation phase

The geophysical survey approach adopted at this phase was the 2-D resistivity imaging technique. For the 2-D survey, the established 30 survey location points that cut across the diverse geological settings in the area (Fig. 1b and c) were combed by deploying both Wenner–Schlumberger and Schlumberger arrays using the ABEM SAS 4000 measuring system. The details of the 2D resistivity imaging data acquisition, processing and interpretation at each occupied locations (Fig. 1b) are discussed in Mogaji et al. (2015b). The typical 2D resistivity imaging obtained from the interpreted

Table 1
Borehole yield rating inventory records of the area.

BH Number	The reference Coordinates		Actual yield from the drilled borehole(m ³ /h)
	LAT	LONG	
1	3°45'44"	101°19'29"	17
2	3°45'48"	101°19'27"	18
3	3°45'45"	101°19'12"	18.7
4	3°43'48"	101°20'05"	14
5	3°43'48"	101°20'01"	14
6	3°47'56"	101°20'21"	21
7	3°42'25"	101°19'53"	14.7
8	3°42'37"	101°19'53"	16.29
9	3°43'10"	101°19'08"	10.72
10	3°45'44"	101°19'15"	6.9
11	4°06'35"	101°20'22"	40
12	3°51'54"	101°16'49"	19.63
13	3°44'42"	101°19'60"	14.06
14	3°44'24"	101°20'02"	2.48
15	3°43'29"	101°20'02"	13.86
16	3°43'27"	101°20'05"	14.01
17	3°46'08"	101°18'42"	20.4
18	3°57'21"	101°11'55"	26.5
19	4°04'15"	101°14'22"	43.71
20	3°44'04"	101°19'56"	18.34
21	3°43'46"	101°19'60"	13.97
22	3°46'51"	101°17'58"	24.41
23	4°04'19"	101°15'04"	20
24	3°57'50"	101°17'44"	33.7
25	3°53'04"	101°28'39"	14.6
26	3°56'18"	101°30'47"	16.6
27	4°52'03"	101°14'11"	0.39
28	3°43'23"	101°30'05"	8.67

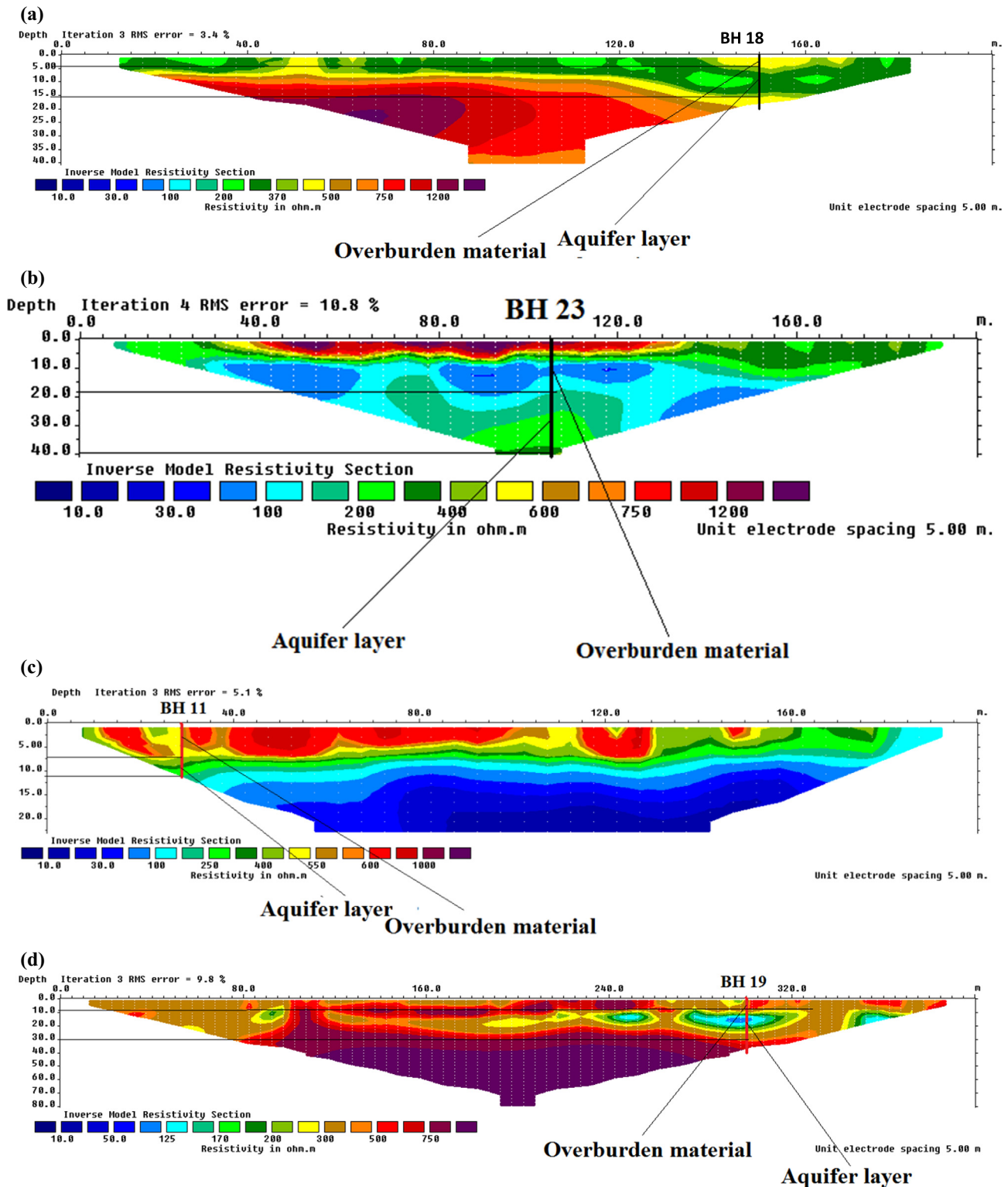


Fig. 3. Examples of the 2D resistivity imaging sections showing how geoelectrical parameters were delineated on the identified rock types in the area. Where a, b, c and d are the sections located on Alluvium, Devonian, Silurian and Igneous rock types, respectively.

data is shown in Fig. 3. Based on this interpretation, the following subsurface parameters including OVR, OVT, ACR, and ACT were determined at each 2-D resistivity imaging location: (Figs. 2 and 3). The summary of the obtained subsurface parameters at each location is presented in Table 2. Afterward, the secondary order parameters often refers to as Dar – Zarrouk Parameters

(DZP) i.e. transverse resistance (TR) via applying the renowned relevant equation (1) according to Maillet (1974) was determined using the interpreted geoelectrical parameters (ρ and h)

$$TR = \sum_{i=1}^n \rho_i h_i = \rho_1 h_1 + \rho_2 h_2 \dots \rho_n h_n \quad (1)$$

Table 2

The interpreted geoelectric and the computed Dar – Zarrouk Parameters (DZP) obtained from the 2-D resistivity sections.

2D LOC	E	N	ACT (m)	ACR (Ω-m)	OVT (m)	OVR (Ω-m)	TR (Ω m ²)
1	463204	745927	13	222	9	94	2886
2	465287	754971	13	464	2	178	6032
3	467594	764259	6	509	3	50	3054
4	463747	772268	14	246	13	126	3444
5	452052	749179	8	241	4	445	1928
6	455548	768295	6	166	35	1202	996
7	445504	736757	21	600	15	359	12,600
8	447858	748279	15	356	20	391	5340
9	450071	748718	22	481	25.1	472	10,582
10	446769	754725	9	500	18	559	4500
11	446051	762713	14	200	23	645	2800
12	437438	744320	11	594	15.4	219	6534
13	437156	762228	15	415	15.7	363	6225
14	430581	780035	16	300	14	201	4800
15	413755	772616	10	257	18	355	2570
16	411097	775646	27	399	15	334	10,773
17	411227	758588	16	170	15	408	2720
18	407504	756097	8	160	15	312	1280
19	428290	752376	22	223	9	222	4906
20	411797	747975	9	227	15	316	2043
21	417238	755739	27	181	11	180	4887
22	433562	737921	32	331	12	86	10,592
23	429776	734188	8	160	73	7	1280
24	416459	736352	26	83	20	251	2158
25	440713	751713	40	750	12	532	30,000
26	427679	759179	37	513	6.2	141	18,981
27	417459	786875	17	798	25	562	13,566
28	447635	771658	29	215	38	562	6235
29	450825	783823	16	1061	5	2301	16,976
30	463794	777484	34	646	5.7	95	21,964

ACT: Aquifer layer thickness, ACR: Aquifer layer resistivity, OVT: Overburden layer thickness, OVR: Overburden layer resistivity, and TR: Transverse resistance.

3.3. Generating the thematic maps of the groundwater potential conditioning factors (GPCFs)

According to Mogaji and Omobude (2017), the factors that are believed to be influencing the occurrence and storage potential of groundwater are referred to as groundwater potential conditioning factors (GPCFs). Based on the discussion above, this study is considering the OVR, OVT, ACR, ACT, Tr, and K. The hydrological significances of these GPCFs have been reported in literatures. To mention few, Oyedele et al. (2011), reported that the resistivity parameter of the weathered formation (aquiferous unit) and the delineated overburden unit thickness have been successfully evaluated for groundwater potential rating in an area. The parameters K and Tr on the other hand, have been established as the major driver of groundwater discharge in an area for they largely determined the variability of groundwater potential from place to place (Okogbue and Omonona, 2013; Ikechukwu, 2012; Tizro et al., 2010; Lee et al., 2012a). However, very few studies have considered the Tr and K factors in spatial modeling of groundwater potentiality and groundwater vulnerability assessment (Adepelumi et al., 2006; Mogaji et al., 2011; Mogaji, 2017). With these aforementioned factors, the direct influence of subsurface stratigraphic layer, physical properties on the conduit movement of groundwater in the subsurface can be effectively evaluated. But then, in order to model multi-criterially these GPCFs in the mechanism of DS-EBF algorithm, their values at the geophysical and hydrogeological measurement points were spatially processed in GIS environment for producing their raster map shown in Fig. 4. The produced Fig. 4 maps were further converted into evidential layers to serve as an input for the multi-criterially DS – EBF model.

3.4. The EBF Model

In reference to our published works Mogaji et al. (2015a, 2016), the theory of this model which has its origin from the Bayesian

generalization was reviewed for this study. Its efficacy in several environmental studies including mineral potential mapping (Moon, 1990; Carranza and Hale, 2002; Carranza et al., 2005), landslide susceptibility (Mohammady et al., 2012; Lee et al., 2012c; Pourghasemi et al., 2013), aquifer vulnerability mapping (Al-Abadi, 2015b) has been documented. The DS-EBF model theory according to Lee et al. (2012c), support four series of mass functions including belief (Bel), disbelief (Dis), uncertainty (Unc) and Plausibility (Pls). The model inbuilt uncertainty functionality according to Park (2010), put it at advantage over other spatial data integration models viz- a – viz its ability to mapping of target zones as well as predicting the degree of uncertainty of the same zones. Exploring this singular attribute of the DS – EBF model in the field of groundwater hydrology, a more precision and biasless groundwater potentiality prediction model map can be produced (Althuwaynee et al., 2012; Lee et al., 2012c).

According to the DS – EBF model basic theory reviewed (Al-Abadi, 2015b; Mogaji et al., 2016), the relationships mapping applications in groundwater vulnerability and groundwater recharge potential mapping have been defined easily using the renowned Eqs. (2)–(7). Thus, they were applied to the prepared GPCFs (Fig. 4) and the groundwater well yield inventory locations to model the GPPI map of the area following procedural approach in Neshat and Pradhan (2015) and Pourghasemi and Beheshtirad (2015) where the weight values for each GPCFs obtainable from the Belief values were calculated and synthesized for the GPPI map construction.

$$\lambda(T_p) = \frac{\frac{N(L \cap E_{ij})}{N(L)}}{\frac{N(E_{ij}) - N(L \cap E_{ij})}{N(A) - N(L)}} \quad (2)$$

where $N(L \cap E_{ij})$: number of groundwater wells that occurred in E_{ij} ; $N(L)$: total number of existed wells with productive yield in the study area; $N(E_{ij})$: number of pixels in the study area.

The Bel function can be calculated as

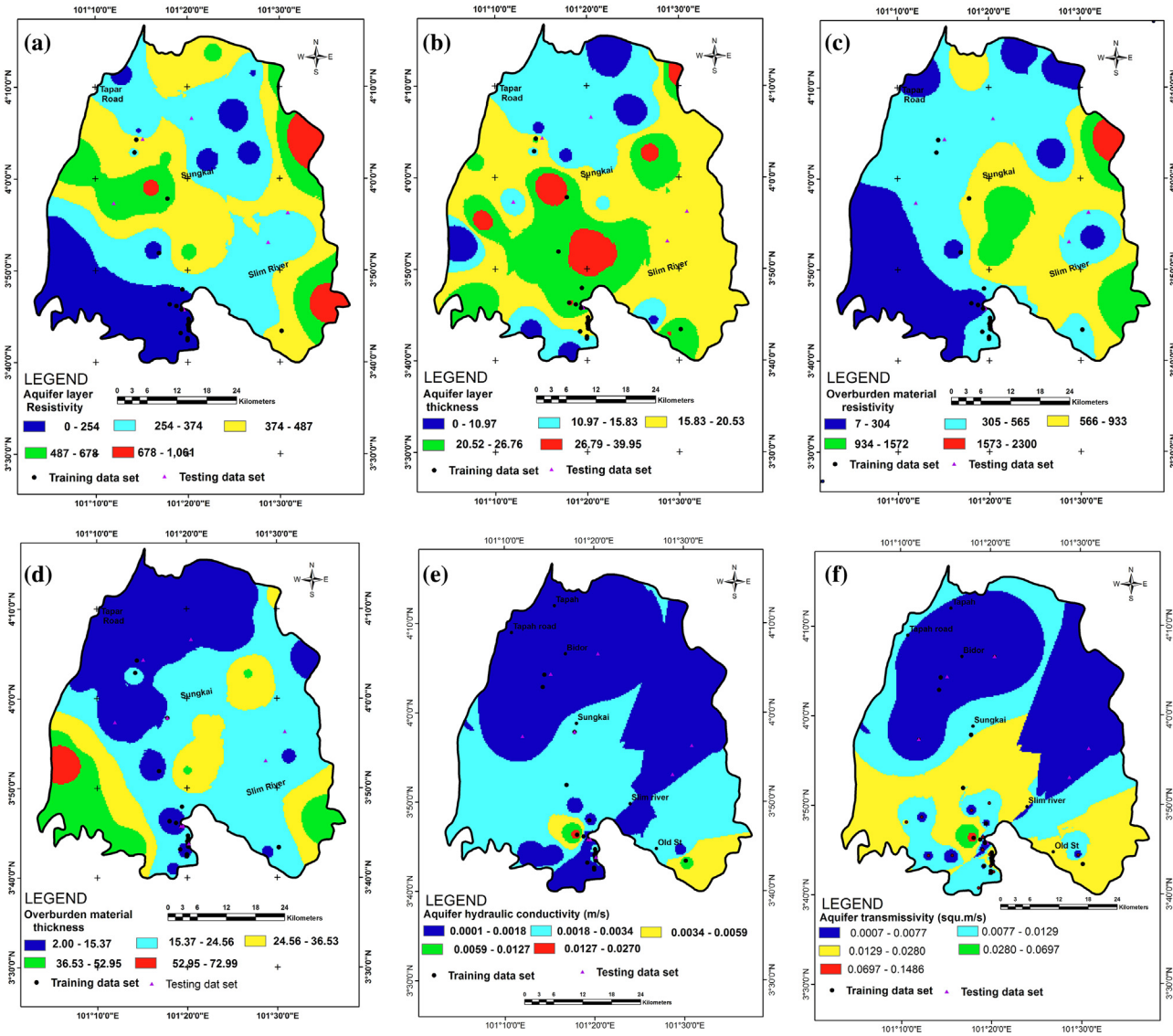


Fig. 4. Groundwater conditioning parameters/factors for the EBF – DST and MCDA-AHP models: (a) Aquifer layer resistivity; (b) aquifer layer thickness; (c) overburden material resistivity; (d) overburden material thickness; (e) aquifer hydraulic conductivity and (f) aquifer transmissivity.

$$Bel = \frac{\lambda(T_p)_{E_{ij}}}{\sum \lambda(T_p)_{E_{ij}}} \quad (3)$$

The likelihood ratio for supporting the opposite target proposition is calculated as

$$\lambda(\bar{T}_p) = \frac{\frac{N(L) - N(L \cap E_{ij})}{N(L)}}{\frac{N(A) - N(L) - N(E_{ij}) + N(L \cap E_{ij})}{N(A) - N(L)}} \quad (4)$$

The Dis function is calculated as

$$Dis = \frac{\lambda(\bar{T}_p)_{E_{ij}}}{\sum \lambda(\bar{T}_p)_{E_{ij}}} \quad (5)$$

The uncertainty (Unc) and the plausibility (Pls) values area were obtained using Eqs. (6) and (7)

$$Unc = 1 - Dis - Bel \quad (6)$$

$$Pls = 1 - Dis \quad (7)$$

By exploring these EBF model's algorithm, the weighted values for the considered GPCFs were determined (Table 3).

4. Results and discussion

4.1. The DS – EBF algorithm applicability result in groundwater mapping

The results of the applied DS – EBF algorithms given in Eqs. (3), (5)–(7) to the spatially modeled groundwater potential conditioning factors (Fig. 4) established the estimate of the following DS – EBF mass series function namely: belief, disbelief, uncertainty, and plausibility as presented in Table 3. According to column 2 and 6 of Table 3, the correlation between groundwater occurrence and aquifer formation (ACR) reflects that resistivity values in the range of 80–254 Ω m and 254–374 Ω m class boundaries have the highest Bel values of 0.83 and 0.1, respectively. Such resistivity class boundaries formation according to Olorunfemi and Fasuyi (1993) typified a saturated formation. This is unlike the class boundaries formation of 678–1061 Ω m that indicate very low saturated unit and characterized with the lowest belief value. This thus revealed that this area high degree of potential storage prospect is relatively in agreement with the DS – EBF modeling output. Further, the ACT estimates in column 2, the class boundaries of 20.53–26.76 m and 26.76–39.95 have highest Bel values of 0.41

Table 3

Spatial relationship between the groundwater potential conditioning parameters (GPCFs) productive groundwater well using DS – EBF model.

The GPCFs Evidential themes	Category (Classes)	Potentiality for groundwater storage prospect	A	B	Belief functions components			
					Bel	Dis	Unc	Pls
Aquifer layer resistivity (ACR)	80–254	High	7906	15	0.83	0.05	0.12	0.95
	254–374	Medium high	15,716	1	0.10	0.23	0.67	0.77
	374–487	Medium	13,855	2	0.08	0.26	0.66	0.74
	487–678	Low	5361	1	0.04	0.28	0.68	0.72
	678–1061	Very low	1556	0	0.00	0.39	0.61	0.61
Aquifer layer thickness (ACT)	8–10.97	Very low	2585	0	0.00	0.41	0.59	0.59
	10.97–15.83	Low	10,549	3	0.16	0.22	0.62	0.78
	15.83–20.53	Medium	19,194	8	0.24	0.20	0.56	0.80
	20.53–26.76	Medium high	9896	7	0.41	0.16	0.43	0.84
	26.76–39.95	High	2170	1	0.27	0.18	0.55	0.82
Aquifer hydraulic conductivity (K)	0.02–0.060	Very low	25,051	8	0.08	0.24	0.68	0.76
	0.060–0.101	Low	17,177	7	0.19	0.20	0.61	0.80
	0.101–0.139	Medium	1860	1	0.24	0.18	0.58	0.82
	0.139–0.195	Medium high	264	2	0.63	0.16	0.21	0.84
	0.195–0.348	High	42	1	0.71	0.12	0.17	0.88
Overburden material resistivity (OVR)	7–304	Medium High	10,507	4	0.31	0.21	0.48	0.79
	304–565	High	18,009	14	0.38	0.08	0.54	0.91
	566–933	Medium	11,254	1	0.07	0.26	0.67	0.74
	933–1572	Low	4059	0	0.00	0.22	0.78	0.78
	1573–2300	Very low	565	0	0.00	0.20	0.80	0.80
Overburden material thickness (OVT)	2.00–15.37	High	13,892	10	0.60	0.11	0.29	0.89
	15.37–24.56	Medium high	18,448	9	0.16	0.19	0.65	0.81
	24.26–36.53	Medium	7291	0	0.00	0.25	0.75	0.75
	36.53–52.95	Low	4150	0	0.00	0.23	0.77	0.77
	52.95–72.99	Very low	613	0	0.00	0.20	0.80	0.80
Aquifer transmissivity (Tr)	0.0007–0.0077	Very low	16,082	7	0.09	0.40	0.51	0.60
	0.0077–0.0129	Low	10,925	6	0.18	0.18	0.64	0.82
	0.0129–0.0280	Medium	10,492	3	0.13	0.22	0.65	0.78
	0.0280–0.0697	Medium high	4592	2	0.20	0.15	0.65	0.85
	0.0697–0.1486	High	2303	1	0.26	0.11	0.63	0.89

A: No of class pixels; B: No of groundwater wells.

and 0.27, respectively (Column 6). Similarly, the class boundary with low ACT value of 8–10.97 m has the lowest Bel value (Column 6). According to [Oladapo et al. \(2009\)](#) and [Mogaji \(2016\)](#), an area underlain with thicker aquifer unit often characterized with high groundwater yield. Thus, the area groundwater potentiality occurrences quite correlated with DS – EBF modeling output of the ACT factor determined. Precisely, the groundwater storage prospect assessment correlation across the other GPCFs such as OVT, OVR, K and Tr show similar trend revelation of the likes of both ACR and ACT results discussed. In addition, the quantitative comparison analysis among the columns 3, 7, 8 and 9 of [Table 3](#) has also indicated groundwater potentiality mapping efficacy of the DS–EBF model. This clue is as numerically interpreted in Column 3 where the area groundwater storage prospect potentiality agreed with the Dis, Unc and Pls results in columns 7, 8 and 9, respectively. The comparison results has quantitatively established that the class boundaries with high Bel values across the modeled geoelectrical-based GPCFs are found to be associated with the low degree values of Dis, Unc and high degree values of Pls. The Dis and Unc component of the DS functional series in accordance with [Mogaji \(2017\)](#) has further confirmed the integrity of Bel index estimate whose both low and higher values are observed correlated with the low and high groundwater potentiality storage prospect interpretations of Column 3 in the area. This result is in agreement with the findings of [Lee et al. \(2012c\)](#) and [Althuwaynee et al. \(2012\)](#).

However, in order to synthesize the hydrogeological significance of these geoelectrical parameters induced GPCFs in [Table 3](#), the multi – criterially functionality of this renowned Dempster's rule of combination algorithms as used in the studies of [Carranza](#)

and [Hale \(2002\)](#), [Mogaji et al. \(2015a\)](#), [Mogaji et al. \(2016\)](#) and [Al-Abadi \(2015b\)](#) were explored. The results of the calculated combined degrees of mass functions/beliefs at each observation location points as depicted in [Fig. 5](#) are presented in [Table 4](#). Moreover, through the efficacy of the geospatial technique GIS software, the results in [Table 4](#) were spatially modeled to produce the integrated maps of DS – EBF model shown in [Fig. 6](#). The spatial correlation analysis of [Fig. 6](#) maps result revealed that zones of high Bel values ([Fig. 6a](#)) are characterized with zones with low Dis ([Fig. 6b](#)), low Unc ([Fig. 6c](#)) and high Pls ([Fig. 6c](#)) values spatially modeled for the area. Thus, having explored the data driven evidential belief function algorithms (Eqs. (3), (5)–(7)), the above analyzed four mass function series (Belief, Disbelief, Uncertainty and Plausibility) supported by the DS – EBF model has presented the quantitative relationships between the groundwater potentiality occurrences and the conditioning factors ([Lee et al., 2012c](#); [Althuwaynee et al., 2012](#); [Nampak et al., 2014](#)).

4.2. The construction of groundwater productivity potentiality map

This study employed the conceptual approach reported in the studies of [Moon \(1990\)](#) and [Tangestani and Moore \(2002\)](#) in constructing the area groundwater potentiality map. This entail the modeling of DS – EBF model-based Bel index values in column 4 of [Table 4](#) computed using Eq. (8). The clue is such that the Bel index among the supported four mass function series of the model, gives a more exact evidence indicating the existence of groundwater reservoir formation occurrence in the area compared to the other mass function series indexes. Thus, through exploiting the spatial analyst module in GIS environment as used in the studies

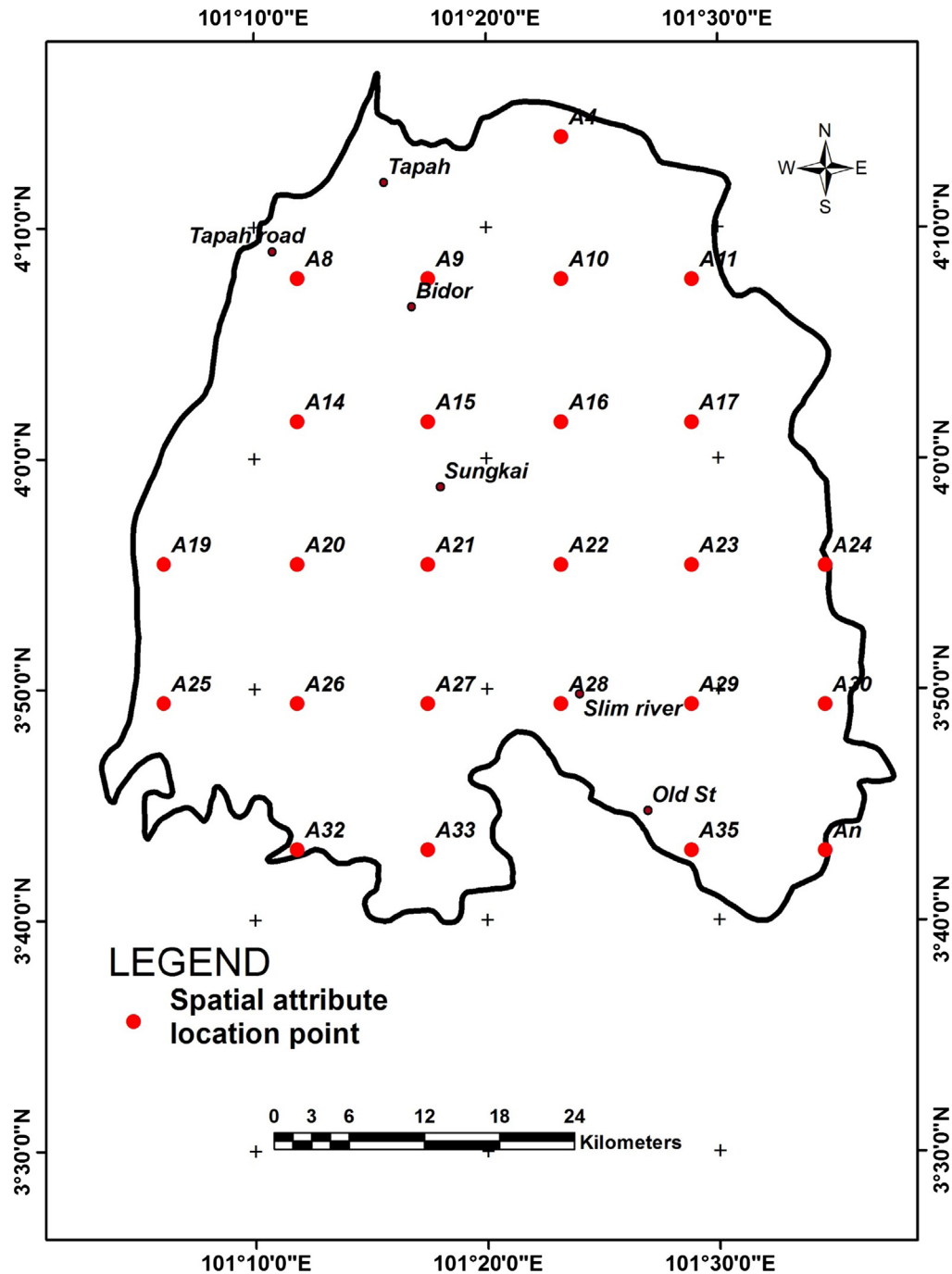


Fig. 5. The evidential and spatial attributes scoring template model used in the study.

of Akinlalu et al. (2017), Mogaji (2017) and Mogaji (2016), the computed Bel index values in column 4 of Table 4 were spatially modeled for constructing the groundwater productivity potentiality index map for the area (Fig. 7).

$$Bel_x = \frac{Bel_A Bel_B + Bel_A Unc_B + Bel_B Unc_A + \dots + Bel Unc_n}{\beta} \quad (8)$$

where, Bel_x : lower degree of belief for each layers of parameters type or range; Unc_x : degree of uncertainty for each layers of parameters type or range; x; the A, B, ..., G denoting each parameters types and $\beta = 1 - Bel_A Dis_B - Dis_A Bel_B$.

4.3. The uncertainty modeling assessment of the area potentiality prediction results

In a means to reduce the level of biasness in the use of the predictive modeling result for the purpose of environmental decision making, the quantification of the degree of the model uncertainty is essential (Feizizadeh et al., 2014). This study explored the capability of the DS – EBF model to model the level of uncertainty degree associated with the predicted potential zones in the investigated area (Fig. 7). Through, the use of the given DS algorithm in Eq. (9), the Unc index values (Column 6 of Table 4) characterizing the area were determined. Applying the Spatial analyst command algorithm in the GIS environment, the degree of uncertainty values

Table 4

Belief functions component indexes computed results for the synthesized GCPs hydrogeologic, evidential themes.

OBS-Points Numbers	Grid Center's coordinates		The belief functions indexes			
	Easting	Northing	Bel	Dis	Unc	Pls
1	754386	468233	0.4699	0.4832	0.0670	0.5368
2	765042	468233	0.5520	0.4068	0.0603	0.6123
3	743978	456834	0.6320	0.3541	0.0564	0.6883
4	754386	456834	0.5658	0.4040	0.0693	0.6351
5	765042	456834	0.0000	0.0574	0.0000	0.0000
6	775451	456834	0.3834	0.5333	0.1369	0.5202
7	733322	445434	0.7699	0.2292	0.0394	0.8093
8	743978	445434	0.6772	0.4063	0.0677	0.7449
9	754386	445434	0.3519	0.5186	0.1452	0.4971
10	765042	445434	0.7869	0.1772	0.0359	0.8228
11	775451	445434	0.3192	0.3124	0.1085	0.4277
12	733322	434034	0.9300	0.2072	0.0397	0.9697
13	743978	434034	0.6772	0.4063	0.0677	0.7449
14	754386	434034	0.2890	0.3464	0.1039	0.3929
15	765042	434034	0.1552	0.4892	0.1410	0.2962
16	775451	434034	0.1791	0.7369	0.1460	0.3251
17	786107	434034	0.3274	0.6288	0.1219	0.4493
18	733322	422883	0.8847	0.2055	0.0378	0.9225
19	743978	422883	0.8669	0.1377	0.0268	0.8937
20	754386	422883	0.4454	0.4569	0.1139	0.5592
21	765042	422883	0.3110	0.5682	0.1208	0.4318
22	775451	422883	0.3035	0.6514	0.1222	0.4257
23	786107	422883	0.2001	0.7453	0.1741	0.3742
24	743978	411235	0.7793	0.1875	0.0333	0.8125
25	754386	411235	0.9812	0.1271	0.0282	1.0094
26	775451	411235	0.7564	0.2384	0.0415	0.7979
27	786107	411235	0.2149	0.7136	0.1603	0.3751

Bel: Belief, Pls: Plausibility; Unc: Uncertainty, Dis: Disbelief and GCPs: Groundwater Conditioning Parameters.

associated with the demarcated potential mapping zones in Fig. 7 were quantitatively evaluated (Table 5). Revealing from Table 5, the percentage level of uncertainty characterizing the predicted potential zones in the area is in the range of 2–17% with $Unc < 10\%$ associated with the mediums and highs potential zones whereas the $Unc > 10\%$ is related with the low potential zones. Generally, all the predicted potential classes revealed by GPPI map (Fig. 7) can be explore for groundwater exploration for the reason of low degree/percentage of uncertainty characterizing them. However, those mapped mediums and highs potential zones with lowest uncertainty degree are more promising for higher groundwater productivity potentiality that will reliably serve as a new leads site for future borehole development in the area. It can thus be implies that based on the area extent coverage estimated for the predicted potential classes (see column 4 of Table 5), about 63% of the area can be explored for groundwater resource development

$$Unc_x = \frac{Unc_A Unc_B + \dots + Unc_n Unc_n}{\beta} \quad (9)$$

where Unc_x degree of uncertainty for each layers of parameters type or range

4.4. The DS – EBF modeling output validation assessment

Assessing the performance efficiency of the multi-criteriality potential of the DS – EBF model involving the geoelectrically and hydrogeologically derived based GPCFs in groundwater potential mapping is considered a clue for establishing the DS – EBF model as a good alternative MCDA model technique in the field of groundwater hydrology. This study employed two approaches in achieving this objective. Firstly, the reacting operating characteristics (ROC) validation technique was explored. With this technique, ROC curve plots was produced using both AcrGIS 10.2 and IDRISI software where the, randomly partitioned bore well location

inventories of ratio 70:30 were spatially analyzed with the DS-EBF-based GPPI map (Fig. 7) for both model training and model testing, respectively. The ROC curve plot has the false positive rate on the X-axis and the true positive rate on the Y-axis as shown in Fig. 8. According to Fig. 8, the area under the curve (AUC) value of 0.888 which implies the 88.8% prediction accuracy rate of the adopted DS – EBF model approach. Secondly, the Dar – Zarrouk Parameter analysis of the delineated aquifer materials properties obtained from the processed and interpreted geophysical 2D resistivity measurement location over the predicted potential zones of the DS-EBF-based GPPI map was determined. This was burned out of the view that the productivity of the predicted potential classes are functions of the hydraulic properties of the underlain aquifers (Soupiou et al., 2007; Shahid et al., 2014). The similar approach of Tizro et al. (2010), Oborie and Udom (2014) and Maillet (1974) employed for determining the transverse resistance (TR); longitudinal conductance (S)), properties of the aquifer units material was explored in this study. Thus, through applying the given Eq. (1), the result of the computed TR for the aquifer unit is as presented in Table 2. According to Table 2, the determined TR values for the aquifer unit were in the range of 996–30,000 $\Omega \text{ m}^2$ (Column (8) of Table 2). With the application GIS – based spatial analyst tool, the associated TR parameter values characterizing the predicted potential classes (Fig. 7) were spatial analyzed. The analyzed results established that the low potential zones have TR values vary from 996 to 13,566 $\Omega \text{ m}^2$ whereas the mediums/high potential classes are characterized with TR values in the range of 1280–30,000 $\Omega \text{ m}^2$. According to Tizro et al. (2010), the aquifer transmissivity (Tr) is directly related to TR which implies that at higher TR, the Tr will also be higher and thus the groundwater potential will be good. Thus, the mapped medium and high potential classed revealed by GPPI map (Fig. 7) are quantitatively characterized with higher groundwater potentiality compared with the low predicted zones. It can be deduced from the two validation approach discussed, that the DZP analyzed results quite agreed

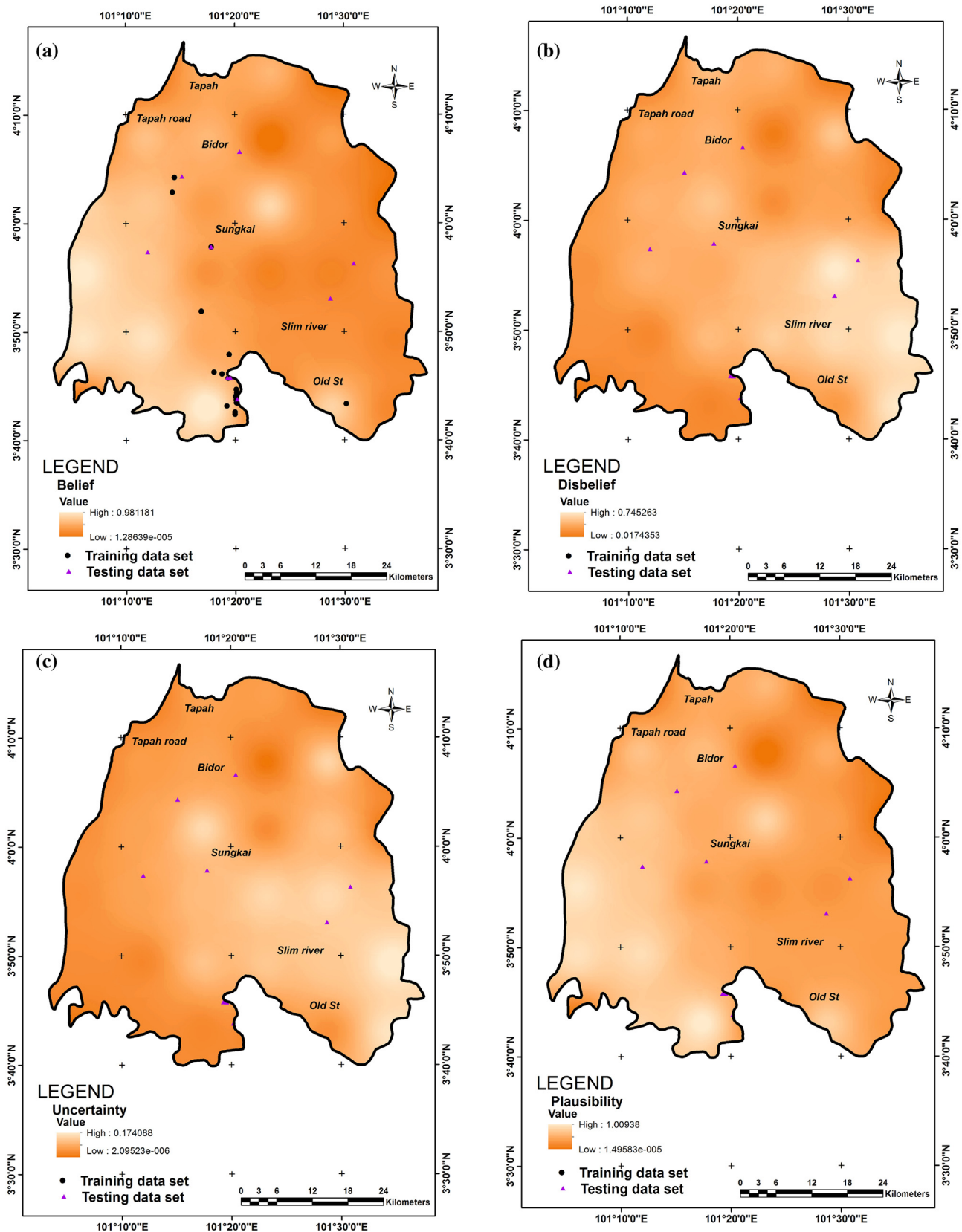


Fig. 6. Integrated results of DS - EBF model; (a) belief, (b) disbelief, (c) uncertainty, (d) plausibility.

with the mapped mediums/high potential classes with the lowest Unc degree quantified. Hence, it is concluded that the map produced by the DS - EBF model exhibited satisfactory result in the

investigated area. Therefore, the predicted mediums/high potential areas are reliable to be explore for groundwater resources development in the study area.

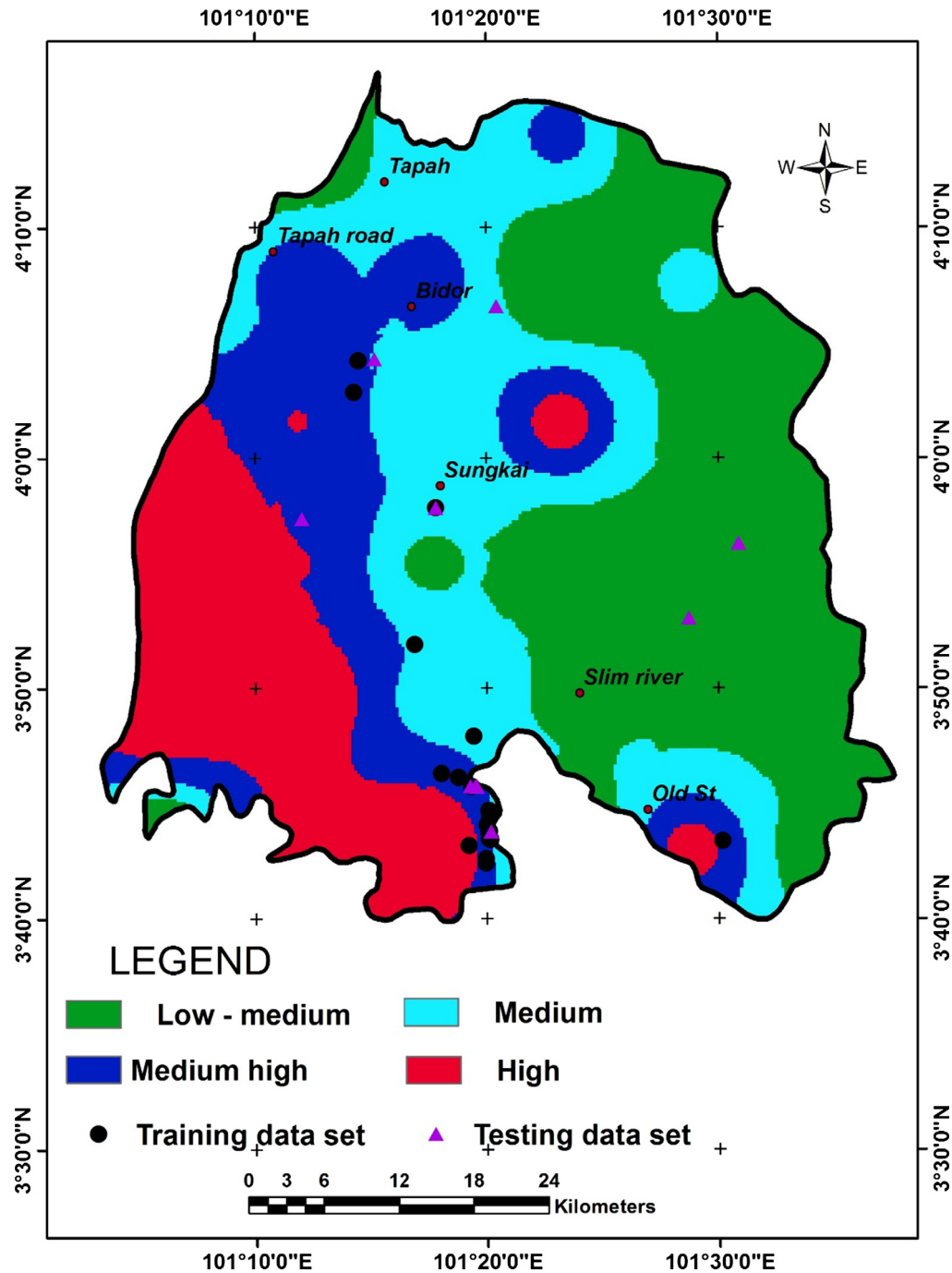


Fig. 7. Groundwater productivity potential index (GPPI) map of the area.

Table 5

The potential zones uncertainty degree quantified analysis and the area coverage extent.

Potential zones Classes	Uncertainty degree Values range	Percentage level of the uncertainty degree	Area Extent km ² (%)
L-M	0.1039–0.1741	10–17%	1064.75 (37)
M	0.0359–0.0809	3–8%	734.54(26)
M-H	0.0359–0.0677	3–6%	533.23(19)
H	0.0268–0.0677	2–6%	532.03(18)

L – M: Low medium, M: Medium, M – H: Medium high and H: High.

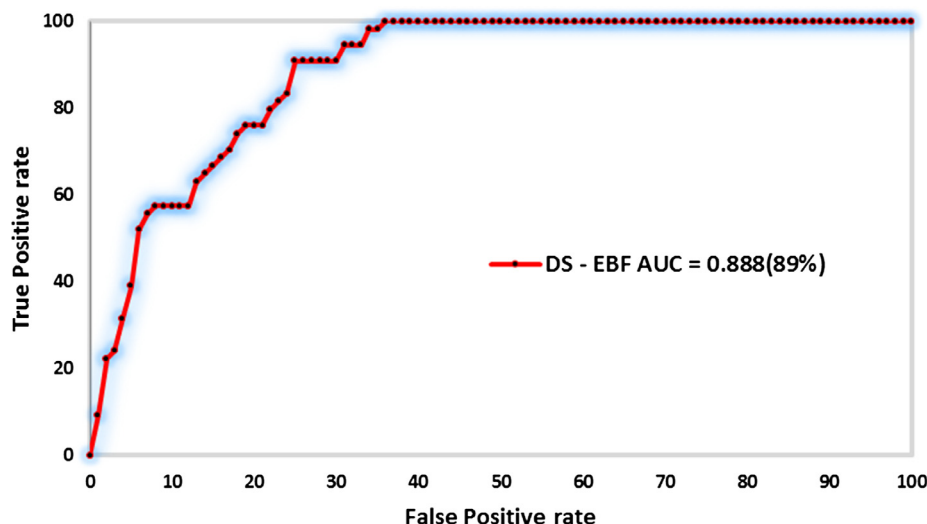


Fig. 8. The ROC technique validation result.

5. Conclusions

In groundwater potential mapping, the used of multi-criterially spatial integration models are promising due to their capability of producing logical accuracy spatial prediction models. But then, the aspect of modeling degree of uncertainty in predictive mapping of promising zones that often reduces predictive model precision and reliability in the field of groundwater hydrology are often trivialized. Thus, this current research is focused on proving the effectiveness of GIS - based Dempster Shafer data driven evidential belief function model (DS - EBF) to addressing this multi-criterially spatially predictive models shortcoming in a given groundwater resource development project. This model was explored using a case study at the Perak province, Malaysia for the purpose of producing reliable environmental decision making tool that can be used for maximizing the optimal exploration of groundwater resources in the area. In order to achieve this research aim, a database consisting of groundwater record data (well locations; yield; transmissivity) and geophysical measurement record data was constructed. Afterward, the proposed model was used to quantitatively establish spatial relationship between the known productive bore well locations and the derived geoelectrically and hydrogeologically induced groundwater potential conditioning factors consisting of aquifer layer thickness, aquifer layer resistivity, overburden material resistivity, overburden material thickness, aquifer hydraulic conductivity and aquifer transmissivity obtained. Based on the likelihood and probabilistic applications of this model's algorithms, four mass function series indexes including the Belief (Bel), Disbelief (Dis), Uncertainty (Unc) and Plausibility (Pls) were determined. The afterward comparative analysis of the integrated degrees of these mass function indexes enabled production of the area groundwater productivity potentiality index (GPPI) map. The analyzed degree of uncertainty over the predicted potential classes revealed by the produced DS-EBF-based GPPI map quantitatively established >10% percentage degree of uncertainty for the predicted low potential zones whereas it is <10% for the predicted mediums/highs potential classes in the area. Furthermore, the efficiency performance evaluation of the DS - EBF model through applications of ROC curve technique provided the model prediction rate of 88.8%. The result of the Dar - Zarrouk Parameter analysis on the delineated aquifer units using the transverse resistance values determined in the range of 1280–30,000 Ω

m^2 revealed the quantitatively the prolificness of the delineated aquifer unit's material within the DS-EBF-based predicted potential zones. With these results of DZP-based transverse resistance and the DS-EBF-based percentage degree of uncertainty for the mediums/highs potential classes of the produced GPPI model map, about 63% of the investigated areas can be reliably explore for groundwater resource development.

In summary, this study results have proven the efficiency of DS - EBF model in the field of groundwater hydrology via producing reliable groundwater potential decision making tool using groundwater potential conditioning factors based on the subsurface data sets induced geoelectric and hydraulic parameters. Thus, this study has wider established the applicability of Dempster - Shafer data driven evidential belief function (DS- EBF) model as a cost-effective approach for improving groundwater resources prospectivity mapping in the field of groundwater hydrology/hydrogeological study. The map obtained by this method can be used by local authorities and water policy makers as a preliminary reference in selecting suitable sites for drilling new boreholes. Thus, considerable contributions to the groundwater literatures can be derived from this research findings.

Acknowledgments

This project was carried out using the financial support from RUI, Investigation of the impacts of summertime monsoon circulation to the aerosols aransportation and distribution in Southeast Asia which can lead to global climate change, 1001/PFIZIK/811228. The authors are equally grateful to Universiti Sains Malaysia (USM) for providng one year Post - Doctoral fellowship Dr. Kehinde Anthony Mogaji (BW001607). Also special appreciation goes to my University back in Nigeria (Federal University of Technology Akure (FUTA) for granting me study leave to utilize the fellowship for research study

References

- Adepelumi, A., Yi-j, M.J., Kim, J.H., Ako, B.D., Son, J.S., 2006. Integration of surface geophysical methods for fracture detection in crystalline bedrocks of southwestern Nigeria. *Hydrogeol. J.* 14, 1284–1306.
- Akinlalu, A.A., Adegbuyiro, A., Adiat, K.A.N., Akeredolu, B.E., Lateef, W.Y., 2017. Application of multi-criteria decision analysis in prediction of groundwater

- resources potential: a case of Oke-Ana, Ilesa Area Southwestern Nigeria. *NRIAG J. Astron. Geophys.*
- Al-Abadi, A.M., 2015a. Groundwater potential mapping at northeastern Wasit and Missan governorates, Iraq using a data-driven weights of evidence technique in framework of GIS. *Environ. Earth Sci.* <https://doi.org/10.1007/s12665-015-4097-0>.
- Al-Abadi, A.M., 2015b. The application of Dempster-Shafer theory of evidence for assessing groundwater vulnerability at Galal Badra basin, Wasit governorate, east of Iraq. *Appl. Water Sci.* <https://doi.org/10.1007/s13201-015-0342-7>.
- Althuwaynee, O.F., Pradhan, B., Lee, S., 2012. Application of an evidential belief function model in landslide susceptibility mapping. *Comput. Geosci.* 44 (2012), 120–135.
- Anomohanran, O., 2015. ScienceDirectHydrogeophysical and hydrogeological investigations of groundwater resources in Delta Central, Nigeria. *J. Taibah Univ. Sci.* 9 (2015), 57–68. <https://doi.org/10.1016/j.jtusci.2014.06.003>.
- Ayazi, M.H., Pirasteh, S., Arvin, A.K.P., Pradhan, B., Nikouravan, B., Mansor, S., 2010. Disasters and risk reduction in groundwater: Zagros Mountain Southwest Iran using geoinformatics techniques. *Disaster Adv.* 3, 51–57.
- Carranza, E.J.M., Hale, M., 2002. Evidential belief function for data-driven geologically constrained mapping of gold potential, Baguio district, Philippines. *Ore Geol. Rev.* 117–132.
- Carranza, E.J.M., Woldai, T., Chikambwe, E.M., 2005. Application of data-driven evidential belief functions to prospectivity mapping for aquamarine-bearing pegmatites, Lundazi District, Zambia. *Nat. Resour. Res.* 14 (1). <https://doi.org/10.1007/s11053-005-4678-9>.
- Corsini, A., Cervi, F., Ronchetti, F., 2009. Weight of evidence and artificial neural networks for potential groundwater mapping: an application to the Mt. Modino area (Northern Apennines, Italy). *Geomorphology* 111, 79–87. <https://doi.org/10.1016/j.geomorph.2008.03.015>.
- Davoodi Moghaddam, D., Rezaei, M., Pourghasemi, H.R., Pourtaghi, Z.S., Pradhan, B., 2013. Groundwater spring potential mapping using bivariate statistical model and GIS in the Taleghan watershed Iran. *Arab. J. Geosci.* <https://doi.org/10.1007/s12517-013-1161-5>.
- Feizizadeh, B., Jankowski, P., Blaschke, T., 2014. A GIS-based spatially-explicit sensitivity and uncertainty analysis approach for multi-criteria decision analysis. *Comput. Geosci.* 64, 81–95.
- Ikechukwu, B.I., 2012. Evaluation of the aquifer hydraulic characteristics from electrical sounding data in Imo River Basin, South Eastern Nigeria: the case of Ogwashi-Asaba Formation. *Int. J. Modern Eng. Res. (IJMER)* 2(5), 3237–3244 (<http://www.ijmer.com>, ISSN: 2249-6645).
- Kaliraj, S., Chandrasekar, N., Magesh, N.S., 2014. Identification of potential groundwater recharge zones in Vaigai upper basin, Tamil Nadu, using GIS-based analytical hierarchical process (AHP) technique. *Arab. J. Geosci.* 7, 1385–1401. <https://doi.org/10.1007/s12517-013-0849-x>.
- Lee, S., Hwang, J., Park, I., 2012c. Application of data-driven evidential belief functions to landslide susceptibility mapping in Jinbu, Korea. *CATENA* 100, 15–30.
- Lee, S.S., Kyo-Young, K., Yongsung, P.I., 2012b. Regional groundwater productivity potential mapping using a geographic information system (GIS) based artificial neural network model. *Hydrogeol. J.*, 1–17 <https://doi.org/10.1007/s10040-012-0894-7>.
- Lee, S., Yong-Sung, K., Hyun-Joo, O., 2012a. Application of a weights-of-evidence method and GIS to regional groundwater productivity potential mapping. *J. Environ. Manage.* 96 (1), 91–105.
- Madan, K.J., Chowdary, V.M., Chowdhury, A., 2010. Groundwater assessment in Salboni Block, West Bengal (India) using remote sensing, geographical information system and multi-criteria decision analysis techniques. *Hydrogeol. J.* 18 (7), 1713–1728. November 2010.
- Magesh, N.S., Chandrasekar, N., Soundranayagam, J.P., 2012. Delineation of groundwater potential zones in Theni district, Tamil Nadu, using remote sensing, GIS and MIF techniques. *Geosci. Front.* 3 (2), 189–219.
- Maillet, R., 1974. The fundamental equations of electrical prospecting. *Geophysics* 12 (4), 529–556.
- Manap, M.A., Sulaiman, W.N.A., Ramli, M.F., Pradhan, B., Surip, N., 2013. A knowledge driven GIS modeling technique for groundwater potential mapping at the Upper Langat Basin, Malaysia. *Arab. J. Geosci.* 6, 1621–1637.
- Mogaji, K.A., Olayanj, G.M., Oladapo, M.I., 2011. Geophysical evaluation of rock types impact on aquifer characterisation in the basement complex areas of Ondo state, Southwestern, Nigeria: Geo-electric assessment and geographic information approach. *Int. J. Water Resour. Environ. Eng.* 3 (4), 77–86.
- Mogaji, K.A., Lim, H.S., Abdullah, K., 2015a. Regional prediction of groundwater potential mapping in a multifaceted geology terrain using GIS-based Dempster-Shafer model. *Arab. J. Geosci.* <https://doi.org/10.1007/s12517-014-1391-1>.
- Mogaji, K.A., Lim, H.S., Abdullah, K., 2015b. Modeling of groundwater recharge using a multiple linear regression (MLR) recharge model developed from geophysical parameters: a case of groundwater resources management. *Environ. Earth Sci.* 2015 (73), 1217–1230. <https://doi.org/10.1007/s12665-014-3476-2>.
- Mogaji, K.A., Omosuyi, G.O., Adelusi, A.O., Lim, H.S., 2016. Application of GIS-based evidential belief function model to regional groundwater recharge potential zones mapping in hardrock geologic terrain. *Environ. Process.* 3 (1), 2016.
- Mogaji, K.A., 2016. Combining geophysical techniques and multi-criteria GIS-based application modeling approach for groundwater potential assessment in southwestern Nigeria. *Environ. Earth Sci.* 75, 1181. <https://doi.org/10.1007/s12665-016-5897-6>.
- Mogaji, K.A., 2017. Development of AHPDST vulnerability indexing model for groundwater vulnerability assessment using hydrogeophysical derived parameters and GIS application. *Pure Appl. Geophys.* <https://doi.org/10.1007/s00024-017-1499-9>.
- Mogaji, K.A., Lim, H.S., 2017. Groundwater potentiality mapping using geoelectrical-based aquifer hydraulic parameters: a GIS-based multi-criteria decision analysis modeling approach. *Terr. Atmos. Ocean. Sci.* 28 (3), 479–500. <https://doi.org/10.3319/TAO.2016.11.01.02>.
- Mogaji, K.A., Omobude, O.B., 2017. Modeling of geoelectric parameters for assessing groundwater potentiality in a multifaceted geologic terrain, Ipinla Southwest, Nigeria – A GIS-based GODT approach. *NRIAG J. Astron. Geophys.*
- Mohammady, M., Pourghasemi, H.R., Pradhan, B., 2012. Landslide susceptibility mapping at golestan province, Iran: a comparison between frequency ratio, Dempster-Shafer, and weights-of-evidence models. *J. Asian Earth Sci.* 61, 221–236.
- Moon, W.M., 1990. Integration of geophysical and geological data using evidential belief function. *IEEE Trans. Geosci. Remote Sens.* 28 (4), 711–720.
- Naghbi, S.A., Pourghasemi, H.R., Pourtaghi, Z.S., Rezaei, A., 2014. Groundwater qanat potential mapping using frequency ratio and Shannon's entropy models in the Moghan watershed, Iraq. *Earth Sci. Inform.* <https://doi.org/10.1007/s12145-014-0145-7>.
- Nampak, H., Pradhan, B., Manap, M.A., 2014. Application of GIS based data driven evidential belief function model to predict groundwater potential zonation. *J. Hydrol.* 513, 283–300.
- Neshat, A., Pradhan, B., Pirasteh, S., Shafri, H.Z.M., 2014. Estimating groundwater vulnerability to pollution using a modified DRASTIC model in the Kerman agricultural area, Iran. *Environ. Earth Sci.* 71, 3119–3131.
- Neshat, A., Pradhan, B., 2015. Risk assessment of groundwater pollution with a new methodological framework: application of Dempster-Shafer theory and GIS. *Nat. Hazards* 10.1007/s11069-015-1788-5.
- Oborue, E., Udom, G.J., 2014. Determination of aquifer transmissivity using geoelectrical sounding and pumping test in parts of Bayelsa State, Nigeria. *J. Phys. Environ. Sci. Res.* 2 (2), 32–40.
- Oh, H.J., Kim, Y.S., Choi, J.K., Park, E., Lee, S., 2011. GIS mapping of regional probabilistic groundwater potential in the area of Pohang City, Korea. *J. Hydrol.* 399, 158–172.
- Oikonomidis, D., Dimogianni, S., Kazakis, N., Voudouris, K., 2015. A GIS/Remote Sensing-based methodology for groundwater potentiality assessment in Tirnavos area, Greece. *J. Hydrol.* 525, 197–208.
- Okogbe, C.O., Omonona, O.V., 2013. Groundwater potential of the Egbe-Mopa basement area, central Nigeria. *Hydrol. Sci. J.* 58 (4), 826–840.
- Oladapo, M.I., Adeoye, O.O., Mogaji, K.A., 2009. Hydrogeophysical study of the groundwater potential of Ilara-Mokin southwestern, Nigeria. *Global J. Earth Sci.* 15(2), 195–204.
- Olorunfemi, M.O., Fasuyi, S.A., 1993. Aquifer types and the geoelectric/hydrogeologic characteristics of part of central basement terrain of Nigeria (Niger State). *J. Afr. Earth Sci.* 16 (3), 309–317.
- Oni, T.E., Omosuyi, G.O., Akinlolu, A.A., 2017. Groundwater vulnerability assessment using hydrogeologic and geoelectric layer susceptibility indexing at Igbara Oke, Southwestern Nigeria. *NRIAG J. Astron. Geophys.* 6, 452–458.
- Oyedele, K.F., Fatuna, O.T., Coker, O.J., 2011. Geophysical assessment of subsurface coastal sediments and their engineering implications. *Arab. J. Geosci.* 4, 543–550.
- Ozdemir, A., 2011a. GIS-based groundwater spring potential mapping in the Sultan Mountains (Konya, Turkey) using frequency ratio, weights of evidence and logistic regression methods and their comparison. *J. Hydrol.* 411, 290–308.
- Ozdemir, A., 2011b. Using a binary logistic regression method and GIS for evaluating and mapping the groundwater spring potential in the Sultan Mountains (Aksehir, Turkey). *J. Hydrol.* 405, 123–136.
- Park, N.W., 2010. Application of Dempster-Shafer theory of evidence to GIS-based landslide susceptibility analysis. *Environ. Earth Sci.* 62 (2), 367–376.
- Pourghasemi, H.R., Moradi, R., Fatemi-Aghda, S.M., Gokceoglu, C., Pradhan, B., 2013. GIS-based landslide susceptibility mapping with probabilistic likelihood ratio and spatial multicriteria evaluation models (North of Tehran, Iran). *Arabian Journal of Geosciences.* <https://doi.org/10.1007/s12517-012-0825-x>.
- Pourghasemi, H.R., Beheshtirad, M., 2015. Assessment of a data-driven evidential belief function model and GIS for groundwater potential mapping in the Koohrang Watershed, Iran. *Geocarto Int.* 30 (6), 662–685. <https://doi.org/10.1080/10106049.2014.966161>.
- Pradhan, B., Neshat, A., Pirasteh, S., Shafri, H.Z.M., 2013. Estimating groundwater vulnerability to pollution using a modified DRASTIC model in the Kerman agricultural area, Iran. *Environ. Earth Sci.* <https://doi.org/10.1007/s12665-013-2690-7>.
- Pradhan, B., 2009. Groundwater potential zonation for basaltic watersheds using satellite remote sensing data and GIS techniques. *Cent. Eur. J. Geosci.* 1, 120–129.
- Rahmati, O., Naser, T., Farhad, N., Saro, L., 2016. Spatial analysis of groundwater potential using weights-of-evidence and evidential belief function models and remote sensing. *Arab. J. Geosci.* 9, 79. <https://doi.org/10.1007/s12517-015-2166-z>.
- Sener, E., Davra, A., Ozcelik, M., 2005. An integration of GIS and remote sensing in groundwater investigation: a case study in Bunduc Turkey. *Hydrogeology* 13 (5), 826–839.
- Shahid, S., Nath, S.K., Kamal, A.S., 2014. GIS integration of remote sensing and topographic data using fuzzy logic for ground water assessment in Midnapur District, India. *Geocarto Int.* 17, 69–74. <https://doi.org/10.1080/10106040208>.

- Soupiou, P.M., Kouli, M., Vallianatos, F., Vafidis, A., Stavroulakids, G., 2007. Estimation of aquifer hydraulic parameters from surface geophysical methods: a case study of Keitis Basin in Chania (Crete - Greece). *J. Hydrol.* 338, 122–131. <https://doi.org/10.1016/j.jhydrol.2007.02.028>.
- Tangestani, M.H., Moore, F., 2002. The use of Dempster-Shafer model and GIS in integration of geoscientific data for porphyry copper potential mapping, north of Shahr-e-Babak, Iran. *Int. J. Appl. Earth Observ. Geoinform.* 4 (1), 65–74.
- Tizro, T.A., Voudouris, K.S., Mashayekhi, M.S., 2010. Hydrogeological framework and estimation of aquifer hydraulic parameters using geoelectrical data: a case study from West Iran. *Hydrogeol. J.* 2010 (18), 917–929. <https://doi.org/10.1007/s10040-010-0580-6>.
- Todd, D.K., Mays, L.W., 2005. *Groundwater Hydrology*. Wiley, NewYork.